



Efficient blue emitters based on 1,3,5-triazine for nondoped organic light emitting diode applications

Jian Liu^a, Ming-Yu Teng^a, Xiao-Peng Zhang^a, Kai Wang^a, Cheng-Hui Li^{a,b,*},
You-Xuan Zheng^{a,*}, Xiao-Zeng You^{a,b,*}

^a State Key Laboratory of Coordination Chemistry, School of Chemistry and Chemical Engineering, Nanjing National Laboratory of Microstructures, Nanjing University, Nanjing 210093, PR China

^b Academician Work Station of Changzhou Trina Solar Energy Co. Ltd., Changzhou 213022, Jiangsu Province, PR China

ARTICLE INFO

Article history:

Received 25 February 2012

Received in revised form 21 May 2012

Accepted 2 June 2012

Available online 25 June 2012

Keywords:

OLED

Nondoped

Triazine

Triphenylamine

Thiophene

ABSTRACT

Two novel efficient blue emitters (**TTT-1**, **TTT-2**) containing 1,3,5-triazine, thiophene and triphenylamine have been designed and synthesized. Organic light emitting diodes (OLEDs) using these new triazine derivatives as emissive layers, ITO/TAPC (60 nm)/**TTT-1** (Device A) or **TTT-2** (Device B) (40 nm)/TPBi (60 nm)/LiF (1 nm)/Al (100 nm), were fabricated and tested. The OLEDs exhibited good performances with low turn-on voltage of 3 V, maximum luminance of ca. 8990 cd/m² for **TTT-1** and 15,980 cd/m² for **TTT-2**, and maximum luminance efficiency of 4.7 cd/A for **TTT-1** and 4.0 cd/A for **TTT-2**, respectively.

© 2012 Elsevier B.V. All rights reserved.

1. Introduction

Organic light-emitting diodes (OLEDs) have attracted much attention due to their promising applications in full-color display panels, flexible displays, and lighting sources [1–7]. Over the past decades, numerous families of fluorescent organic compounds have been studied as the emitting materials in OLEDs, with the aim to optimize the device performance through modifying their conjugation, morphology, and electron/hole mobility [8–12]. However, many fluorescent organic compounds used in OLEDs suffer from “concentration quenching” effect in solid state and unbalanced carrier mobility (the hole mobility is generally several orders higher than electron mobility), lead-

ing to low quantum efficiency of the device [13,14]. Therefore, new materials with nonplanar structures (to prevent orderly molecular packing and consequently alleviate the fluorescence quenching) and high electron transporting capability (to balance the carrier mobility) are crucial in creating high efficient OLEDs [15].

In this study, we designed and synthesized new fluorescent organic compounds (**TTT-1**, **TTT-2**) containing triazine, triphenylamine and thiophene building blocks. The 1,3,5-triazine unit is a typical electron-accepting unit and have been frequently incorporated into the backbone of conjugated compounds to improve their electron-injection and electron-transportation abilities [16–27]. Introduction of the bulky and nonplanar triphenylamine moiety has been shown to be effective in preventing orderly molecular packing, improving the glass-transition temperature (T_g) and increasing the hole-transporting properties [28]. The thiophene unit is popularly used in optoelectronic materials due to its remarkable optic, electronic and redox properties [29]. A combination of these three functional moieties is rarely reported in the literature and would be

* Corresponding authors. Address: State Key Laboratory of Coordination Chemistry, School of Chemistry and Chemical Engineering, Nanjing National Laboratory of Microstructures, Nanjing University, Nanjing 210093, PR China.

E-mail addresses: chli@nju.edu.cn (C.-H. Li), yxzheng@nju.edu.cn (Y.-X. Zheng), youxz@nju.edu.cn (X.-Z. You).

effective to construct new fluorescence emitters with good carrier-transport property and high solid-state emission efficiency. As expected, non-doped devices employing our new fluorescent organic compounds as emitters display very competitive performances at low operating voltage. Particularly, to the best of our knowledge, the performances of OLED device based on **TTT-2** are among the best ever reported for blue OLEDs based on triazine derivatives either with or without a dopant.

2. Experimental section

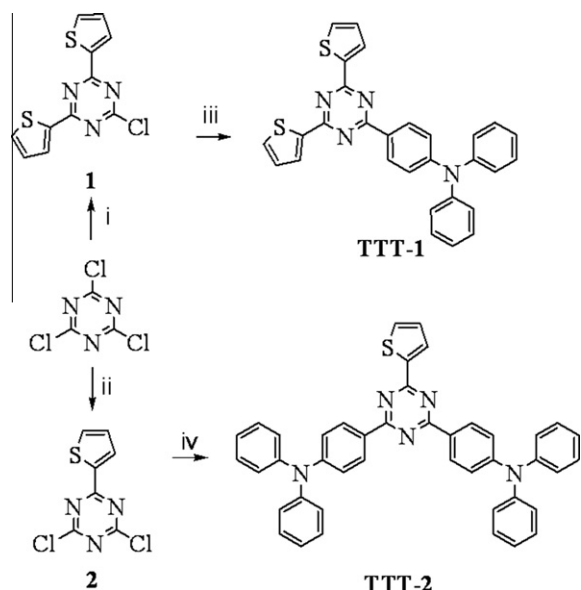
2.1. Materials

All reactions were performed under argon and were magnetically stirred. THF was distilled from sodium and benzophenone prior to use. Commercially available reagents were used without further purification unless otherwise stated. Column chromatography was carried out using flash silica gel (300–400 mesh). The chemical structures and synthetic routes of **TTT-1** and **TTT-2** are shown in Scheme 1.

2.2. Synthetic procedure

2.2.1. Synthesis of 2-chloro-4,6-di(thiophen-2-yl)-1,3,5-triazine (**1**)

A solution of 2-bromothiophene (1.63 g, 10 mmol) in anhydrous THF (20 mL) was added dropwise to a suspension of iodine-activated magnesium (0.29 g, 12 mmol) in anhydrous THF (10 mL) over 30 min. After complete addition, the reaction mixture was stirred and refluxed for 3 h and then cooled to room temperature. The resulting Grig-



Scheme 1. (i) 3 equiv. 2-thienylmagnesium bromide, 50 °C, 12 h; (ii) 1.5 equiv. 2-thienylmagnesium bromide, 25 °C, 12 h; (iii) 1.5 equiv. 4-diphenylaminophenylboronic acid, K_2CO_3 , $Pd(dppf)Cl_2$, dioxane, H_2O , 90 °C, 12 h; (iv) 2.4 equiv. 4-diphenylaminophenylboronic acid, K_2CO_3 , $Pd(dppf)Cl_2$, dioxane, H_2O , 90 °C, 12 h.

nard solution was added dropwise to a solution of cyanuric chloride (0.61 g, 3.3 mmol) in anhydrous THF (20 mL) at 0–10 °C. The mixture was stirred for 10 h at 50 °C and then poured into ice water (50 mL) and extracted twice with CH_2Cl_2 (100 mL). The organic phases were combined, washed with water and brine, dried over anhydrous sodium sulfate, and then concentrated. The residue was purified by flash chromatography on silica gel (hexane/EA 20:1) to afford **1** (0.6 g, 65%) as a white solid. mp 149–151 °C; IR (KBr) ν 732, 810, 1257, 1421, 1473, 1521 cm^{-1} ; 1H NMR ($CDCl_3$, 500 MHz): δ 8.28 (d, $J_1 = 4.0$ Hz, $J_2 = 1.0$ Hz, 2H), 7.71 (d, $J_1 = 5.0$ Hz, $J_2 = 1.0$ Hz, 2H), 7.24 (d, $J_1 = 5.0$ Hz, $J_2 = 4.0$ Hz, 2H); ^{13}C NMR ($CDCl_3$, 500 MHz) δ 169.06, 160.33, 139.65, 134.06, 133.28, 128.81. FAB (m/z): 279 (M^+). Anal. Calcd for $C_{11}H_6ClN_3S_2$: C, 47.22; H, 2.16; N, 15.02. Found: C, 47.12; H, 2.21; N, 14.98.

2.2.2. Synthesis of 2,4-dichloro-6-(thiophen-2-yl)-1,3,5-triazine (**2**)

This compound was prepared similarly to **1** except that the ratio of 2-bromothiophene to cyanuric chloride is 1.5 while the Grignard reaction temperature is 25 °C. Compound **2** was obtained as a white solid in 68% yield. mp 152–153 °C; IR (KBr) ν 787, 847, 1030, 1248, 1335, 1420, 1508 cm^{-1} ; 1H NMR ($CDCl_3$, 500 MHz): δ 8.30 (d, $J_1 = 4.0$ Hz, $J_2 = 1.0$ Hz, 1H), 7.80 (d, $J_1 = 5.0$ Hz, $J_2 = 1.0$ Hz, 1H), 7.25 (d, $J_1 = 5.0$ Hz, $J_2 = 4.0$ Hz, 1H); ^{13}C NMR ($CDCl_3$, 500 MHz) δ 171.63, 170.19, 137.98, 136.17, 135.09, 129.30. FAB (m/z): 230.9 (M^+). Anal. Calcd for $C_7H_3Cl_2N_3S$: C, 36.23; H, 1.30; N, 18.11. Found: C, 36.17; H, 1.25; N, 18.15.

2.2.3. Synthesis of **TTT-1**

To a stirred solution of compound **1** (0.558 g, 2 mmol) in 1,4-dioxane (60 mL) was added 4-diphenylaminophenylboronic acid (0.867 g, 3 mmol), potassium carbonate (1.24 g, 9 mmol), H_2O (15 mL), and $Pd(dppf)Cl_2$ (0.080 g, 0.1 mmol). The resulting mixture was stirred at 90 °C under argon atmosphere for 12 h. The solvent was evaporated under reduced pressure and the residue was treated with water (80 mL), extracted twice with CH_2Cl_2 (50 mL \times 3). The organic phases were combined and washed twice with water and once with brine, dried over anhydrous sodium sulfate. After removing the solvent under reduced pressure, the residue was loaded onto silica gel column with PE/EA (20/1, v/v) as eluent to give a yellow solid (0.615 g, 63%). mp 182–183 °C; IR (KBr) ν 711, 813, 1172, 1278, 1373, 1506, 1589 cm^{-1} ; 1H NMR ($DMSO-d_6$, 500 MHz): δ 8.42 (d, $J = 9.0$ Hz, 2H), 8.28 (dd, $J_1 = 3.5$ Hz, $J_2 = 1.5$ Hz, 2H), 8.00 (dd, $J_1 = 5.0$ Hz, $J_2 = 1.5$ Hz, 2H), 7.42–7.44 (m, 4H), 7.33 (dd, $J_1 = 5.0$ Hz, $J_2 = 3.0$ Hz, 2H), 7.18–7.23 (m, 6H), 7.03 (d, $J = 9.0$ Hz, 2H); ^{13}C NMR ($DMSO-d_6$, 500 MHz) δ 170.58, 167.53, 152.24, 146.50, 141.35, 134.19, 132.30, 130.59, 130.39, 129.48, 127.10, 126.27, 125.34, 120.07. FAB (m/z): 488.1 (M^+). Anal. Calcd for $C_{29}H_{20}N_4S_2$: C, 71.28; H, 4.13; N, 11.40. Found: C, 71.19; H, 4.23; N, 11.32.

2.2.4. Synthesis of **TTT-2**

TTT-2 was prepared similarly to **TTT-1** except that **1** was replaced by **2** while the ratio of 4-diphenylaminophenylboronic acid to **2** is 3. **TTT-2** was obtained as a yellow solid in

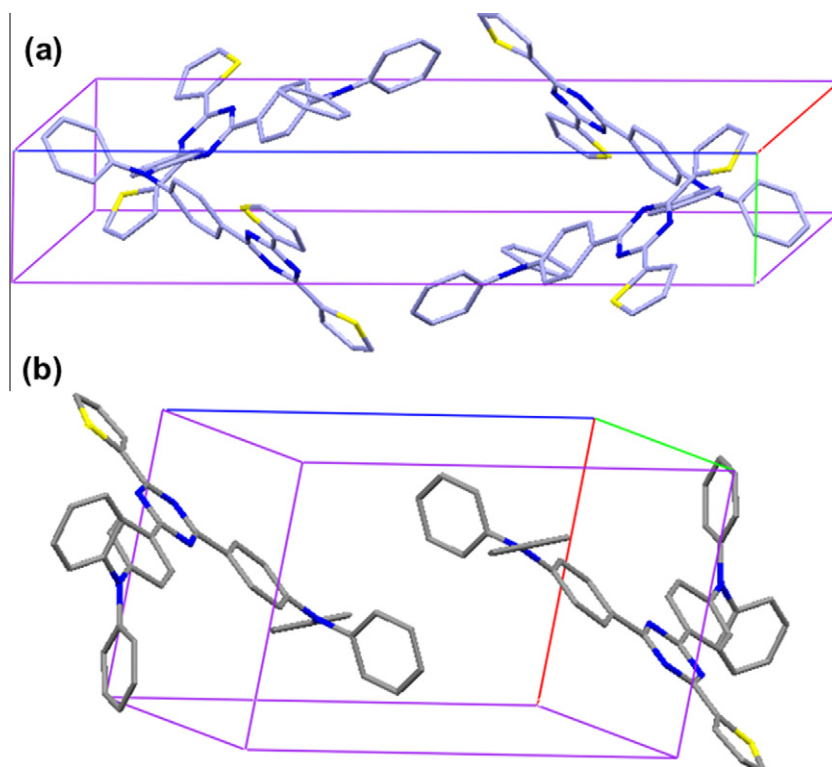


Fig. 1. The molecular packing diagram of **TTT-1** (a) and **TTT-2** (b).

59% yield. mp 233–235 °C; IR (KBr) ν 696, 816, 1174, 1369, 1489, 1589 cm^{-1} ; ^1H NMR (DMSO- d_6 , 500 MHz): δ 8.44 (d, $J = 9.0$ Hz, 2H), 8.28 (dd, $J_1 = 3.5$ Hz, $J_2 = 1.0$ Hz, 2H), 7.96 (dd, $J_1 = 5.0$ Hz, $J_2 = 1.0$ Hz, 2H), 7.39–7.42 (m, 8H), 7.31 (dd, $J_1 = 5.0$ Hz, $J_2 = 3.5$ Hz, 2H), 7.17–7.21 (m, 12H), 7.01 (d, $J = 9.0$ Hz, 2H); ^{13}C NMR (CDCl_3 , 500 MHz) δ 170.33, 167.50, 151.79, 146.97, 131.61, 130.95, 130.13, 129.51, 128.71, 128.33, 125.64, 124.14, 121.07. FAB (m/z): 649.2 (M^+). Anal. Calcd for $\text{C}_{43}\text{H}_{31}\text{N}_5\text{S}$: C, 79.48; H, 4.81; N, 10.78. Found: C, 79.39; H, 4.85; N, 10.66.

2.3. Measurements

Melting points were measured on a Melt-Temp apparatus and are uncorrected. Infrared spectra were recorded in KBr pellet on a vector 22 Bruker spectrophotometer in the range of 4000–400 cm^{-1} . ^1H NMR and ^{13}C NMR were recorded using a Bruker spectrometer at 500 MHz using TMS as an internal standard. Low and high resolution mass spectra were recorded using an EIT-OF-MS spectrometer in FAB mode. Elemental analyses of the compounds were performed on a Perkin-Elmer 240 analyzer. Absorption spectra were recorded on a Shimadzu UV-3100 spectrometer. Emission spectra were recorded on a Hitachi F-4600 luminescence spectrometer upon excitation at 313 nm. Cyclic voltammetry (CV) was performed on an Im6eX electrochemistry working station. All CV measurements were carried out in anhydrous CH_2Cl_2 containing 0.1 M TBAP as a supporting electrolyte, purging with argon prior to conduct the experiment. Platinum electrode, Ag/AgCl in saturated

KCl (aq.) and a platinum wire were used as working electrode, reference electrode and counter electrode, respectively. Differential scanning calorimetry (DSC) analyses were performed on a METTLER TOLEDO modulating-DSC-823 Low-Temperature Difference Scanning Calorimeter. The samples were first heated to melt and then cooled to 25 °C before the DSC measurement at 5 °C/min. Thermogravimetric analyses (TGA) were collected on a Perkin-Elmer Pyris 1 TGA analyzer with a heating rate of 10 °C/min under nitrogen.

2.4. EL device fabrication and electro-optical characterization

All OLEDs with the emission area of 0.1 cm^2 were fabricated on the pre-patterned ITO-coated glass substrate having an ITO sheet resistance of 15 Ω/sq . Substrates were cleaned by sequentially ultrasonication in detergents and in deionized water, followed by UV ozone treatments. The stack of organic layers consists of a thin layer of TAPC (60 nm) as the hole-transport layer, **TTT-1** or **TTT-2** (40 nm) as emitting layer and TPBi (60 nm) as the electron-transport layer. The Al cathode (100 nm) was then prepared by evaporation of Al after LiF of (1 nm) was deposited. All chemicals used for EL devices were sublimed in vacuum prior to use. The vacuum was less than 1×10^{-5} Pa during all materials deposition. For the hole-only devices, a thin layer of appointed compound (120 nm) was deposited onto ITO substrate pretreated with UV ozone, followed by Al (100 nm) deposition. For the electron-only devices, a thin layer of BCP (10 nm) was evaporated as the

hole-blocking layer on ITO (no pretreatment with UV ozone). Layers of appointed compound (120 nm), LiF (1 nm) and Al (100 nm) were then sequentially deposited. The current density–voltage–luminance characteristics, current efficiency and power efficiency versus current density of the devices were measured with a computer controlled KEITHLEY 2400 source meter with a calibrated silicon diode in air without device encapsulation. On the basis of the uncorrected EL spectra, the Commission Internationale de l'Eclairage (CIE) coordinates were calculated using a test program of the Spectra scan PR650 spectrophotometer.

3. Results and discussion

3.1. Synthesis and characterization

Grignard reaction between 2,4,6-trichloro-1,3,5-triazine and 2-thienylmagnesium bromide affords the intermediates (**1**, **2**), which were coupled with 4-diphenylaminophenylboronic acid via Suzuki reaction to yield the desired compound (**TTT-1**, **TTT-2**), respectively. Both triazine derivatives were prepared by simple reactions, which is an important factor for commercialization. These compounds were fully characterized by ^1H NMR, ^{13}C NMR (see Supplementary Data), mass spectrometry, and elemental analysis.

Crystals of **TTT-1** and **TTT-2** suitable for X-ray crystallographic analysis were obtained by slow evaporation over a period of 3 weeks of their hexane/EA solution. **TTT-1** and **TTT-2** crystallize in monoclinic space group $P2_1/c$ and triclinic space group $P-1$, respectively. The molecular structure and crystal packing diagram of them are shown in Fig. S1 and Fig. 1. The triazine moieties are almost coplanar to three aryl rings on all sides in these two compounds. There is no π – π stacking interaction between the neighboring molecules due to the large steric hindrance of the nonplanar triphenylamine groups.

3.2. Thermal properties

The thermal property and the morphological stability of **TTT-1** and **TTT-2** were investigated by thermogravimetric analysis (TGA) and differential scanning calorimetry (DSC), respectively. The decomposition temperatures (T_d) corresponding to 5% weight loss are 330 °C for **TTT-1** and 393 °C for **TTT-2**, respectively (Fig. S2). The higher thermal stability of **TTT-2** in comparison with **TTT-1** is due to that organic compounds with higher content of thiophene units are more susceptible to thermal degradation. In the first heating–cooling cycle of DSC study, melting endotherm peaks were observed at 185 °C for **TTT-1** and 240 °C for **TTT-2**, respectively (Fig. 2). However, no endotherm peaks corresponding to glass transition temperatures (T_g) was observed. The cooling curves are flat and show no crystallization. The glass transition temperatures (80 °C for **TTT-1** and 115 °C for **TTT-2**) and recrystallization temperatures (170 °C for **TTT-1** and 210 °C for **TTT-2**) were detected in the second and subsequent heating–cooling cycles. Interestingly, a new melting point at 192 °C was observed for **TTT-1** in the second and subsequent heating–cooling

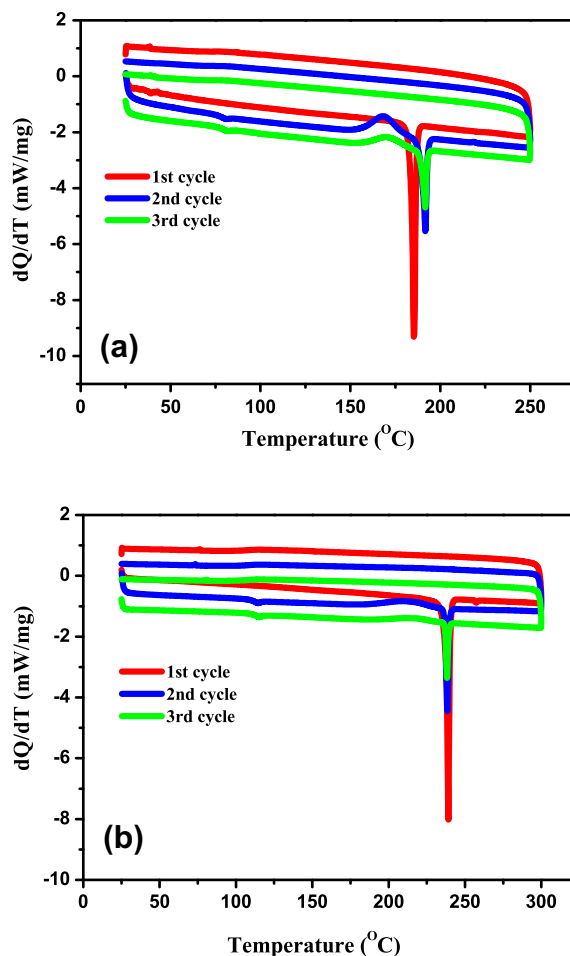


Fig. 2. DSC curves of **TTT-1** (a) and **TTT-2** (b) at a heating (cooling) rate of 5 °C/min. Three heating–cooling cycles are shown, with the first, second, and third cycle represented by red, blue, and green line, respectively. (For interpretation of the references to colour in this figure legend, the reader is referred to the web version of this article.)

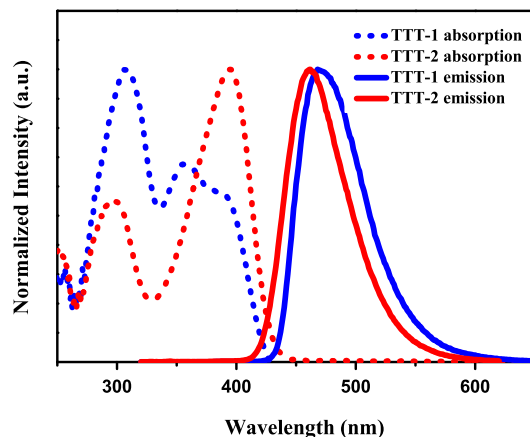


Fig. 3. Absorption and photoluminescence spectra of **TTT-1** and **TTT-2** in dioxane solutions.

cycles, probably due to the formation of new crystalline phase after heating.

Table 1
Physical Properties of **TTT-1** and **TTT-2**.

Compound	$\lambda_{\text{abs,max}}^a$ (nm)	$\lambda_{\text{em,max}}^a$ (nm)	$\lambda_{\text{em,max}}^b$ (nm)	E_g (eV) ^c	HOMO (eV) ^d	LUMO (eV) ^e	T_g (°C)	T_m (°C)	T_d (°C)
TTT-1	308, 356, 390	468	472	2.88	-5.81	-2.93	80	185	330
TTT-2	296, 395	462	467	2.77	-5.78	-3.01	115	240	393

^a 1×10^{-5} M in dioxane.

^b Vacuum deposited thin film.

^c Estimated from the onset wavelengths of the optical absorption.

^d Calculated from the oxidation potentials.

^e Calculated from the HOMO energy levels and E_g .

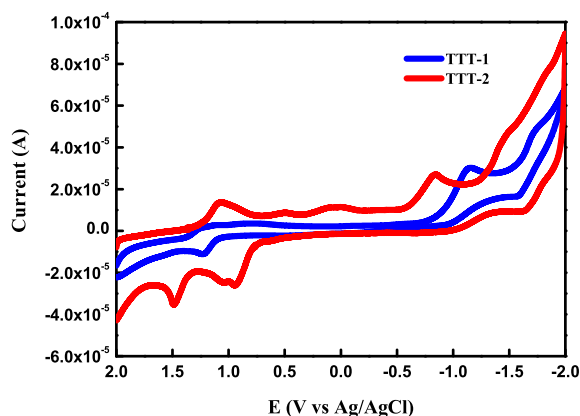


Fig. 4. Cyclic voltammogram of **TTT-1** and **TTT-2** in CH_2Cl_2 solutions (1×10^{-3} M).

3.3. Photophysical properties

The photophysical properties of **TTT-1** and **TTT-2** in both 1,4-dioxane solution (Fig. 3) and thin solid film (Fig. S3) were characterized by UV-vis and photoluminescence (PL) spectra, and the data are summarized in Table 1. As shown in Fig. 3, the UV-Vis spectrum of **TTT-1** shows two peaks at 308 and 356 nm, and a shoulder at 390 nm. The peak at 308 nm originates from the triazine-thiophene units, while the peak at 356 nm comes from the triphenylamine group [30–32]. According to the frontier orbital calculations (see Section 3.5), the low energy shoulder can be assigned to the intra-molecular charge transfer (ICT) transitions from the electron-donating triphenylamine moiety to the electron-accepting triazine-thiophene moiety. For **TTT-2**, the absorption maximum (296 nm) is blue-shifted while the absorption intensity is reduced for π - π^* transitions within the triazine-thiophene units, in accordance with the less thiophene unit in **TTT-2**. Similarly, the opposite changes (red-shift in absorption maximum and increase in absorption intensity) are observed for π - π^* transitions within the triphenylamine units. Therefore, the π - π^* transitions within the triphenylamine units overlaps with the ICT transitions in **TTT-2** and appears as an intense single band at 395 nm. The absorption spectra of thin films (Fig. S3) of **TTT-1** and **TTT-2** are almost the same to those in 1,4-dioxane solution, indicating that there is no significant intermolecular interaction in the films.

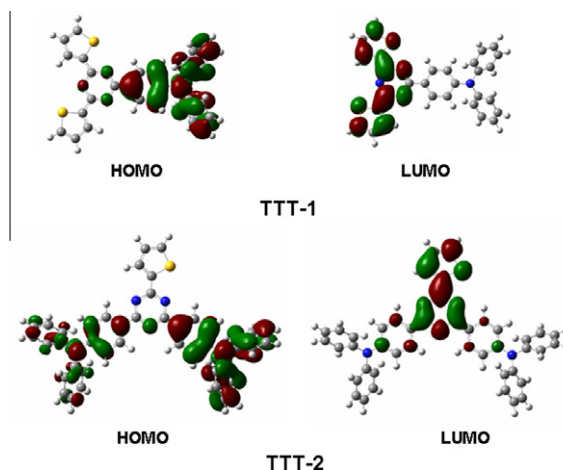


Fig. 5. The calculated HOMO and LUMO levels of **TTT-1** and **TTT-2**.

TTT-1 and **TTT-2** show blue emissions both in dilute 1,4-dioxane solutions and in the solid films when excited at 313 nm (Fig. 3 and Fig. S3). The stoke's shift for **TTT-1** is larger than that for **TTT-2**, indicating a smaller structural distortion in the excited state of **TTT-2** due to the rigidity and steric hindrance of two triphenylamine groups. This is evidenced by the low temperature emission spectra (Fig. S4) where the structural distortion are frozen out at 77 K, resulting in blue-shifted emission energies and similar stoke's shift for **TTT-1** and **TTT-2**. The quantum yields are 0.47 and 0.48 for **TTT-1** and **TTT-2**, respectively, using quinine sulfate monohydrate ($\Phi_{313\text{nm}} = 0.54$) in 0.1 M H_2SO_4 as a standard [33]. It is worth noting that the PL spectra in the solid films of these two compounds exhibit no distinct bathochromic shift in comparison with those in solutions, suggesting that the excited states of **TTT-1** and **TTT-2** could have a similar conjugation length in both states [9].

3.4. Electrochemical properties

Cyclic voltammetry experiments were conducted on **TTT-1** and **TTT-2** at room temperature to investigate their electrochemical properties (Fig. 4). Both quasi-reversible oxidation and reduction process were observed in CH_2Cl_2 solutions with 0.1 M $n\text{-Bu}_4\text{NClO}_4$ (TBAP) as a supporting electrolyte. These quasi-reversible reductive and oxidative behaviors indicate that **TTT-1** and **TTT-2** possess both hole- and electron-transporting characteristics. As shown

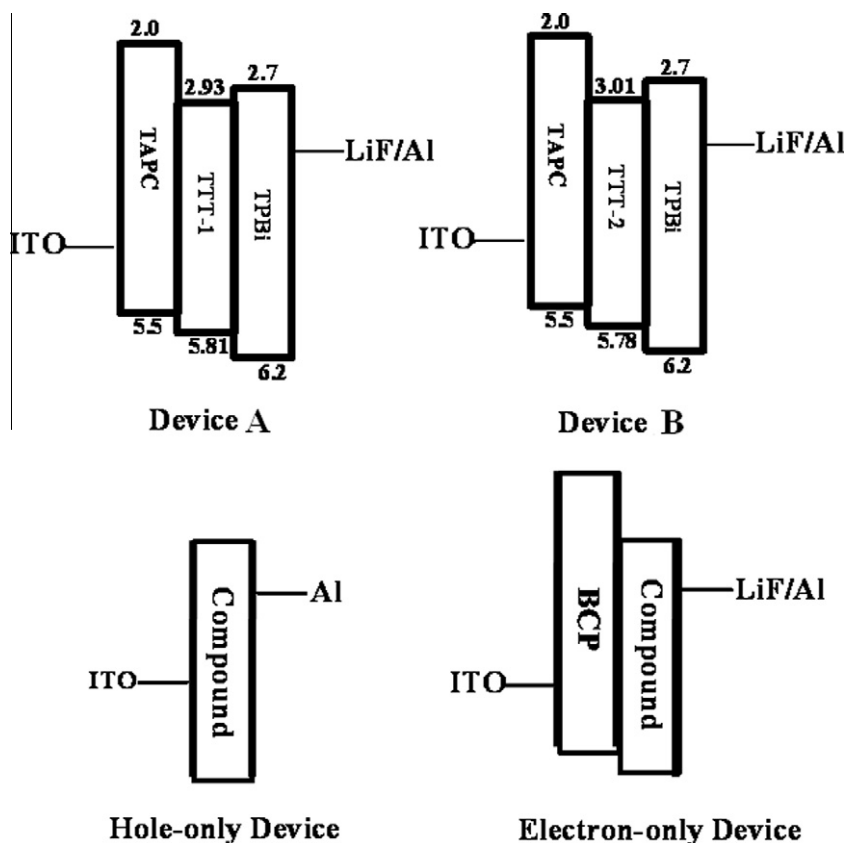


Fig. 6. Energy diagrams of the devices.

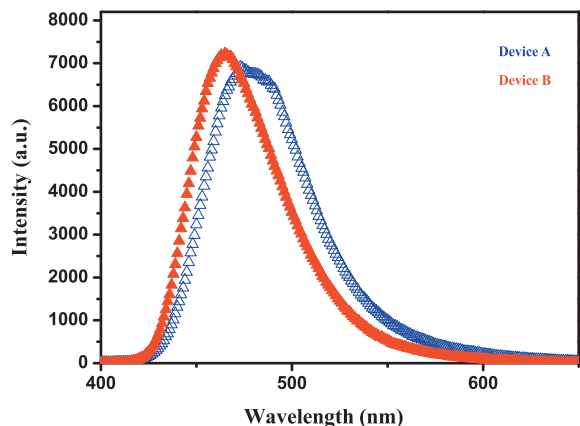


Fig. 7. EL spectra of devices A and B.

in Fig. 4, the oxidation potential of **TTT-1** is higher than that of the **TTT-2**. This is due to that **TTT-2** has more electron-donating triphenylamine groups which reduce the electron affinity of triazine moiety thus lower the oxidation potential. The HOMO energy levels relative to the vacuum level were calculated by using the onset oxidation potential (after being converted to the potential relative to the standard hydrogen electrode potential, NHE) and the Ag/AgCl energy level of -4.44 eV (relative to the

vacuum level) as the standard [34]. The band gaps were estimated from the absorption spectra (absorption edge) of the compounds. The LUMO energy level was calculated from the values of band gap and HOMO energy. The data are summarized in Table 1.

3.5. Density functional theory calculations

All calculations were carried out with Gaussian 03 programs [35]. The geometries of the organic dyes were fully optimized by B3LYP method without any symmetry constraint. The calculations were carried out using the 6-31 g(d,p) basis set for all the atoms. DFT calculations manifest that the HOMO orbital of **TTT-1** and **TTT-2** are located on triphenylamine while LUMO orbitals are located on triazine-thiophene moieties (Fig. 5).

3.6. EL properties of devices based on **TTT-1** and **TTT-2**

To investigate the potential applications of these new blue emitters, two non-doped OLEDs, ITO/TAPC (60 nm)/**TTT-1** (Device A) or **TTT-2** (Device B) (40 nm)/TPBi (60 nm)/LiF (1 nm)/Al (100 nm), have been fabricated (Fig. 6) [36]. The device A shows one sky-blue electroluminescence (EL) band centered at 473 nm while the device B exhibits blue EL band centered at 465 nm (Fig. 7), with CIE coordinates of (0.14, 0.24) and (0.14, 0.16), respectively. The emission energies are very close to those of PL

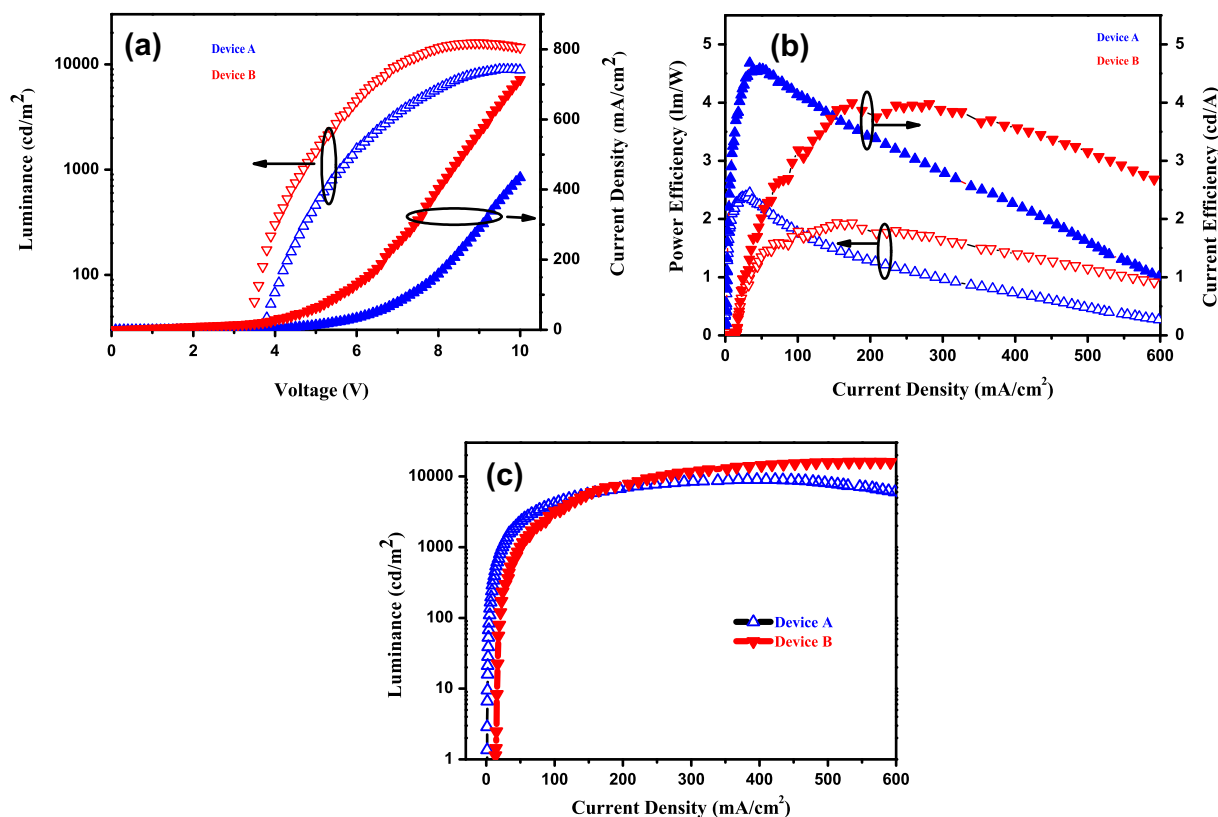


Fig. 8. Characteristics of devices A and B: (a) *L-V-J* characteristics. (b) Current efficiency and power efficiency versus current density of the devices. (c) *L-J* characteristics.

observed for each blue fluorophore in the thin film state (Table 1 and Fig. S3), indicating that there is no exciplex formation at the interface of hole-transporting and light emitting layers. Similar results have been reported previously and can be elucidated by the small difference in energy between the HOMO levels [37].

Current density–voltage–luminance (*J-V-L*) characteristics of each device are presented in Fig. 8. The maximum luminance of the **TTT-1** based device reaches ca. 8990 cd/m^2 with maximum current efficiency (η_c) and power efficiency (η_p) of 4.7 cd/A and 2.4 lm/W , respectively. For OLED based on **TTT-2**, the maximum luminance (ca. 15,980 cd/m^2) is higher while the maximum current efficiency and power efficiency (4.0 cd/A and 1.9 lm/W , respectively) are slightly lower than the **TTT-1** based device. These differences are due to the additional triphenylamine moiety in **TTT-2**, which can enhance the hole mobility. Both devices have a low turn-on voltage around 3 V. All these features are very competitive to other excellent non-doped OLEDs based on fluorescent organic compounds reported previously [38,39].

In order to investigate the carrier-transport behaviors of the **TTT-1** and **TTT-2**, the hole-only devices (ITO/Compound (NPB, TAPC, **TTT-1** or **TTT-2**) (120 nm)/Al (100 nm)) and electron-only devices (ITO/BCP (10 nm)/Alq₃, **TTT-1** or **TTT-2** (120 nm)/LiF (1 nm)/Al (100 nm)) have been also fabricated (Fig. 6) [40]. We chose the popular hole- or electron-transport materials of NPB, TAPC and Alq₃ as the

standards to compare the carrier-transport behaviors of our compounds. Fig. S5 depicts the current vs. voltage characteristics of the hole-only and electron-only devices. The results show that **TTT-1** and **TTT-2** have both hole- and electron-transport abilities as we expected, although their carrier-transport abilities are lower than those of NPB, TAPC and Alq₃. Because of the introduction of two strong electron-donating triphenylamine moieties, the hole-transport ability of **TTT-2** is higher than that of **TTT-1**. Contrarily, the electron-transport ability of **TTT-1** is better than that of **TTT-2** due to its higher electron affinity as manifested in the cyclic voltammetry study [41].

4. Conclusion

In summary, we have designed and synthesized two new fluorophores containing triazine, triphenylamine and thiophene building blocks. These two triazine derivatives exhibited efficient photophysical and electronic properties. OLEDs based on these compounds exhibited good device performances. Because they have both hole- and electron-transport abilities, they are also potential bipolar host materials for the applications in OLEDs.

Acknowledgments

This work was supported by the National Basic Research Program of China (2011CB933303, and 2011CB808704), the

National Natural Science Foundation of China (21021062, 91022031 and 20971067).

Appendix A. Supplementary data

Supplementary data associated with this article can be found, in the online version, at <http://dx.doi.org/10.1016/j.orgel.2012.06.013>.

References

- [1] C.W. Tang, S.A. VanSlyke, *Appl. Phys. Lett.* 51 (1987) 913.
- [2] A.C. Grimsdale, K.L. Chan, R.E. Martin, P.G. Jokisz, A.B. Holmes, *Chem. Rev.* 109 (2009) 897.
- [3] J. Kido, M. Kimura, K. Nagai, *Science* 267 (1995) 1332.
- [4] S.F. Service, *Science* 310 (2006) 1762.
- [5] K. Müllen, U. Scherf, *Organic Light-Emitting Devices: Synthesis, Properties and Applications*; Wiley-VCH Verlag GmbH & Co. KGaA: Weinheim (2006).
- [6] M.A. Baldo, D.F. O'Brien, Y. You, A. Shoustikov, S. Sibley, M.E. Thompson, S.R. Forrest, *Nature* 395 (1998) 151.
- [7] Y.C. Zhu, L. Zhou, H.Y. Li, Q.L. Xu, M.Y. Teng, Y.X. Zheng, J.L. Zuo, H.J. Zhang, X.Z. You, *Adv. Mater.* 23 (2011) 4041.
- [8] A. Kraft, A.C. Grimsdale, A.B. Holmes, *Angew. Chem. Int. Ed.* 37 (1998) 402.
- [9] K.-T. Wong, T.S. Hung, Y. Lin, C.-C. Wu, G.-H. Lee, S.-M. Peng, C.H. Chou, Y.O. Su, *Org. Lett.* 4 (2002) 513.
- [10] H. Park, J. Lee, I. Kang, H.Y. Chu, J.-I. Lee, S.K. Kwon, Y.-H. Kim, *J. Mater. Chem.* 22 (2012) 2695.
- [11] M. Shimizu, K. Mochida, Y. Asai, A. Yamatani, R. Kaki, T. Hiyama, N. Nagai, H. Yamagishi, H. Furutani, *J. Mater. Chem.* 22 (2012) 4337.
- [12] Y.-H. Chen, S.-L. Lin, Y.-C. Chang, Y.-C. Chen, J.-T. Lin, R.-H. Lee, W.-J. Kuo, R.-J. Jeng, *Org. Electron.* 13 (2012) 43.
- [13] B.M. Krasovitskii, B.M. Bolotin, *Organic Luminescent Materials* (V.G. Vopian, Trans.), VCH, Weinheim, Germany, 1988.
- [14] C.-T. Chen, C.-L. Chiang, Y.-C. Lin, L.-H. Chan, C.-H. Huang, Z.-W. Tsai, C.-T. Chen, *Org. Lett.* 5 (2003) 1261.
- [15] B. Valeur, *Molecular Fluorescence*, Wiley-VCH, Weinheim, Germany, 2002.
- [16] H. Zhong, E. Xu, D. Zeng, J. Du, J. Sun, S. Ren, B. Jiang, Q. Fang, *Org. Lett.* 10 (2008) 709.
- [17] J. Pang, Y. Tao, S. Freiberg, X.-P. Yang, M. D'Iorio, S. Wang, *J. Mater. Chem.* 12 (2002) 206.
- [18] J.-W. Kang, D.-S. Lee, H.-D. Park, Y.-S. Park, J.W. Kim, W.-I. Jeong, K.-M. Yoo, K. Go, S.-H. Kim, J.-J. Kim, *J. Mater. Chem.* 17 (2007) 3714.
- [19] A.P. Kulkarni, C.J. Tonzola, A. Babel, S.A. Jenekhe, *Chem. Mater.* 16 (2004) 4556.
- [20] H. Inomata, K. Goushi, T. Masuko, T. Konno, T. Imai, H. Sasabe, J.J. Brown, C. Adachi, *Chem. Mater.* 16 (2004) 1285.
- [21] J.M. Lupton, L.R. Hemingway, I.D.W. Samuel, P.L. Burn, *J. Mater. Chem.* 10 (2000) 867.
- [22] R. Fink, Y. Heischkel, M. Thelakkat, H.-W. Schmidt, C. Jonda, M. Hueppauff, *Chem. Mater.* 10 (1998) 3620.
- [23] R. Fink, C. Frenz, M. Thelakkat, H.-W. Schmidt, *Macromolecules* 30 (1997) 8177.
- [24] T.-Y. Chu, M.-H. Ho, J.-F. Chen, C.H. Chen, *Chem. Phys. Lett.* 415 (2005) 137.
- [25] F.A. Zhong, R.F. Chen, J. Yin, G.H. Xie, H.F. Shi, T. Tsuboi, W. Huang, *Chem. Eur. J.* 17 (2011) 10871.
- [26] G.A. Wen, Y. Xin, X.R. Zhu, W.J. Zeng, R. Zhu, J.C. Feng, Y. Cao, L. Zhao, L.H. Wang, W. Wei, B. Peng, W. Huang, *Polymer* 48 (2007) 1824.
- [27] R. Kannan, G.S. He, T.C. Lin, P.N. Prasad, R.A. Vaia, L.S. Tan, *Chem. Mater.* 16 (2004) 185.
- [28] Y. Shirota, *J. Mater. Chem.* 10 (2000) 1.
- [29] L.F. Perepichka, D.F. Perepichka, *Handbook of Thiophene-based Materials: Applications in Organic Electronics and Photonics*, 2 Volume Set, Wiley-VCH Verlag GmbH & Co. KGaA, Weinheim, 2009.
- [30] P. Leriche, F. Piron, E. Ripaud, P. Frère, M. Allain, J. Roncali, *Tetrahedron Lett.* 50 (2009) 5673.
- [31] F. Riobé, P. Grosshans, H. Sidorenkova, M. Geoffroy, N. Avarvari, *Chem. Eur. J.* 15 (2009) 380.
- [32] R. Sander, V. Stümpflen, J. H. Wendorff, A. Greiner, *Macromolecules* 29 (1996) 7705.
- [33] J.N. Demasa, G.A. Crosby, *J. Phys. Chem.* 76 (1971) 1071.
- [34] J. Pommerehne, H. Vesweber, W. Guess, R.F. Mahrt, H. Bassler, M. Porsh, J. Daub, *Adv. Mater.* 7 (1995) 551.
- [35] M.J. Frisch, G.W. Trucks, H.B. Schlegel, G.E. Scuseria, M.A. Robb, J.R. Cheeseman, Jr. J.A. Montgomery, T. Vreven, K.N. Kudin, J.C. Burant, J.M. Millam, S.S. Iyengar, J. Tomasi, V. Barone, B. Mennucci, M. Cossi, G. Scalmani, N. Rega, G.A. Petersson, H. Nakatsuji, M. Hada, M. Ehara, K. Toyota, R. Fukuda, J. Hasegawa, M. Ishida, T. Nakajima, Y. Honda, O. Kitao, H. Nakai, M. Klene, X. Li, J.E. Knox, H.P. Hratchian, J.B. Cross, C. Adamo, J. Jaramillo, R. Gomperts, R. E. Stratmann, O. Yazyev, A.J. Austin, R. Cammi, C. Pomelli, J.W. Ochterski, P.Y. Ayala, K. Morokuma, G.A. Voth, P. Salvador, J.J. Dannenberg, V.G. Zakrzewski, S. Dapprich, A.D. Daniels, M.C. Strain, O. Farkas, D.K. Malick, A.D. Rabuck, K. Raghavachari, J.B. Foresman, J.V. Ortiz, Q. Cui, A.G. Baboul, S. Clifford, J. Cioslowski, B.B. Stefanov, G. Liu, A. Liashenko, P. Piskorz, I. Komaromi, R.L. Martin, D.J. Fox, T. Keith, M.A. Al-Laham, C. Y. Peng, A. Nanayakkara, M. Challacombe, P.M.W. Gill, B. Johnson, W. Chen, M.W. Wong, C. Gonzalez, J.A. Pople, *Gaussian 03* (2003).
- [36] TAPC here denotes N-(4-(1-(4-(dip-tolylamino)phenyl)cyclohexyl)-phenyl)-4-methyl-N-p-tolylbenzenamine and TPBi is 2,2''-(1,3,5-phenylene)tris(1-phenyl-1H-benzimidazole). ITO is an indium-tin oxide-coated glass.
- [37] S.-L. Lin, L.-H. Chan, R.-H. Lee, M.-Y. Yen, W.-J. Kuo, C.-T. Chen, R.-J. Jeng, *Adv. Mater.* 20 (2008) 3947.
- [38] S. Tao, Z. Peng, X. Zhang, P. Wang, C.-S. Lee, S.-T. Lee, *Adv. Funct. Mater.* 15 (2005) 1716.
- [39] P.I. Shih, C.Y. Chuang, C.H. Chien, E.W.G. Diau, C.F. Shu, *Adv. Funct. Mater.* 17 (2007) 3141.
- [40] A.J. Heeger, I.D. Parker, Y. Yang, *Synth. Met.* 67 (1994) 23.
- [41] M.S. Liu, X. Jiang, S. Liu, P. Herguth, A.K.-Y. Jen, *Macromolecules* 35 (2002) 3532.